



Allergologia et immunopathologia

Sociedad Española de Inmunología Clínica,
Alergología y Asma Pediátrica

www.all-imm.com



ORIGINAL ARTICLE

OPEN ACCESS



SIRT3 improves alveolar epithelial cell damage caused by bronchopulmonary dysplasia through deacetylation of FOXO1

Lili Zang^{a#}, Jinghan Chi^{b#}, Sitong Bi^a, Yi Tao^b, Rong Wang^b, Lihua Li^{a*}

^aDepartment of Children, Beijing Luhe Hospital, Capital Medical University, Beijing, China

^bDepartment of NICU, Senior Department of Pediatrics, the Seventh Medical Center of PLA General Hospital, Beijing, China

[#]Contributed equally

Received 30 June 2022; Accepted 15 December 2022

Available online 1 March 2023

KEYWORDS

apoptosis;
bronchopulmonary
dysplasia;
forkhead box
protein O1;
oxidative stress;
sirtuin 3

Abstract

Background: Bronchopulmonary dysplasia (BPD) is a serious and long-term lung condition commonly observed in premature babies. Sirtuin 3 (SIRT3) has been reported to reduce pulmonary injury and pulmonary fibrosis.

Objective: The present study investigated the specific role of SIRT3 in BPD by establishing hyperoxia-induced BPD rat and cell models. Hematoxylin and eosin staining was used to observe pathological changes in lung tissues.

Materials and methods: The expression levels of SIRT3 and forkhead box protein O1 (FOXO1), as well as its acetylation levels, were detected in hyperoxia-induced lung tissues and cells by Western blot analysis and reverse transcription-quantitative polymerase chain reaction (RT-qPCR). Levels of reactive oxygen species, superoxide dismutase, and malondialdehyde were assessed by using biochemical kits. Following SIRT3 overexpression, the levels of inflammatory cytokines were assessed by RT-qPCR. Apoptosis was determined by terminal deoxynucleotidyl transferase dUTP nickend labeling (TUNEL) and Western blot analysis. Upon FOXO1 knockout, cell inflammation, oxidative stress and apoptosis were evaluated again.

Results: Compared to the control group, the SIRT3 and FOXO1 expression levels were decreased and the FOXO1 acetylation levels were increased in hyperoxia-induced lung tissues and cells. In addition, SIRT3 reduced hyperoxia-induced inflammation, oxidative stress, and apoptosis in A549 cells, and inhibited FOXO1 acetylation to activate FOXO1. However, FOXO1 knockdown reversed the effects of SIRT3 overexpression in hyperoxia-induced A549 cells.

Conclusion: SIRT3 relieved alveolar epithelial cell damage caused by BPD via deacetylation of FOXO1, suggesting that SIRT3 could be a therapeutic target in BPD.

© 2023 Codon Publications. Published by Codon Publications.

*Corresponding author: Lihua Li, Department of Children, Beijing Luhe Hospital, Capital Medical University, No. 82 Xinhua South Road, Tongzhou District, Beijing 101149, China. Email address: lilihua202219@163.com

<https://doi.org/10.15586/aei.v51i2.710>

Copyright: Zang L, et al.

License: This open access article is licensed under Creative Commons Attribution 4.0 International (CC BY 4.0). <http://creativecommons.org/>

Introduction

As one of the common respiratory diseases in premature infants, bronchopulmonary dysplasia (BPD) is mainly characterized by alveolar dysplasia. The main pathological features of BPD are small number and large size of alveoli, accompanied by pulmonary microvascular dysplasia. The long-term outcomes of BPD mainly include recurrent respiratory tract infection, airway hyperresponsiveness, and abnormal lung function.^{1,2} Despite improvement in BPD symptoms by glucocorticoid therapy, hyperoxia, and gentle mechanical ventilation, prolonged hyperoxia induction can lead to lung injury and adversely affect the growth and development of a newborn.^{3,4} Alveolar epithelial cells (AECs) can contribute to the formation of alveolar structures and the air-blood barrier, thus benefiting the normal development of the alveoli.⁵ Previous studies have shown that damage to AECs is a key mechanism of BPD-related lung epithelial injury.^{6,7} Therefore, reducing damage to AECs and maintaining AECs functioning are essential for reducing BPD in preterm infants.

Sirtuin 3 (SIRT3) is a mitochondrial deacetylase that maintains respiratory functions.⁸ The protective role of SIRT3 in lung injury, lung fibrosis, and lung cancer has been reported in the literature.⁹⁻¹¹ In addition, a previous study has revealed that SIRT3 inhibits mitochondrial DNA damage and apoptosis in AECs.¹² Inflammation, apoptosis, DNA damage, and oxidative stress damage in AECs are considered to be the main causes of BPD.¹³⁻¹⁶ The aforementioned studies have suggested that SIRT3 may exert a protective role in damage to AECs caused by BPD; however, the exact mechanism remains unknown.

Forkhead box protein O1 (FOXO1) is a transcription factor that belongs to the FOXO family.¹⁷ Previous studies have confirmed the suppressive role of FOXO1 signaling pathway in non-small cell lung cancer and lung injury.^{18,19} A previous study has demonstrated a significant decrease in FOXO1 expression in the lung tissues after 14 days of induction of hyperoxia.²⁰ Furthermore, microRNA-486 protects against cytotoxicity to reduce damages to human alveolar epithelial A549 cells by targeting phosphatase and tensin homolog (PTEN) and FOXO1 proteins.²¹ However, it is unknown whether FOXO1 protects against damages to AECs caused by BPD. SIRT3 has been proposed to inhibit the acetylation of FOXO1 to activate FOXO1, inhibit inflammation and apoptosis in HK-2 cells, and suppress nonalcoholic fatty liver diseases.^{22,23}

Therefore, the present study established hyperoxia-induced rat and cell models of BPD. The purpose of the study was to examine whether SIRT3 could combine with FOXO1 to attenuate its damage to AECs in hyperoxia-induced model of BPD and discuss the related mechanism. The present data may provide a novel approach and theoretical basis for treating BPD-triggered damage to AECs.

Materials and Methods

Animal model

Neonatal Wistar rats (weight, 4.00 ± 0.43 g; age, 2-3-day old) were randomly divided into two groups ($n = 6$ in each

group, with a total of 12 rats): control and model groups. Neonatal rats in the model group were housed in an environment of 90% oxygen (O_2), <5% carbon dioxide (CO_2), and 60% humidity in a sealed Plexiglas chamber with continuous oxygen monitoring for 14 consecutive days at $25 \pm 2^\circ C$ to establish a hyperoxia-induced model.²⁴ Concentration of oxygen in the control group was controlled at 21%, and the remaining factors were the same as those employed in the model group. Then rats were sacrificed with pentobarbital sodium (90 mg/kg intraperitoneal injection). All animal experiments were in compliance with the Laboratory Animal Ethics Committee regulations of Beijing Luhe Hospital (Beijing, China) and were reported in accordance with the Animal Research: Reporting of In Vivo Experiments (ARRIVE) guidelines.²⁶

Cell culture and treatment

Human respiratory epithelium A549 cells were supplied by Wuhan Sunncell Biotech Co. Ltd. (Cat. No. SNL-089). Cells were cultured in Dulbecco's Modified Eagle Medium (DMEM; Sigma-Aldrich; Merck KGaA) containing 10% fetal bovine serum (Absin, Shanghai, China) and 1% penicillin-streptomycin (both 100 U/mL), and placed in a humid incubator with 5% CO_2 at $37^\circ C$. In order to construct a hyperoxia-induced cell model, A549 cells were cultured for 6 h at $37^\circ C$ in a humidified environment with 95% O_2 and 5% CO_2 in a specially designed hyperoxia cell culture chamber.²⁴ Cells in the control group were incubated continuously for 6 h at $37^\circ C$ in a humidified environment with 21% O_2 and 5% CO_2 .

Cell transfection

PcDNA3.1 overexpression vector (GenScript) encoding the full-length SIRT3 for overexpression of SIRT3 (OV-SIRT3, NC_051336) or the empty plasmid (OV-NC), and small interference (si)RNAs targeting FOXO1 (siRNA-FOXO1-1/2) and its negative control (siRNA-NC) were provided by BioVector NTCC Inc. A total of 20 nM siRNA-FOXO1-1/2, siRNA-NC, OV-SIRT3 and OV-NC were transfected in A549 cells (10^7 cells) by using Lipofectamine® 2000 (Thermo Fisher Scientific Inc.) according to the manufacturer's instructions. RT-qPCR and Western blot analysis were used to detect the transfection efficiency 24 h after transfection. Following the above transfection, the cells were then induced with hyperoxia.

Hematoxylin and eosin (H&E) staining

The rats in the model group were anesthetized with pentobarbital sodium (30 mg/kg by intraperitoneal injection), and then sacrificed. The inferior lobe of the right lung tissues were removed by rapidly opening the chest cavity under aseptic conditions and fixed in 4% formaldehyde at room temperature for 48 h. After being subjected to gradient alcohol dehydration for 2 min each time and xylene transparency, the tissues were embedded in paraffin wax, and 4-mm paraffin sections were prepared. After dewaxing for two times in xylene and rehydrating in gradient

ethanol, the tissues were placed in distilled water for 5 min and stained with hematoxylin for 10 min. After rinsing of the sections for 1 h, they were placed in distilled water, dehydrated in gradient alcohol for 10 min, and stained with 1% eosin alcohol for 3-5 min. The stained sections were dehydrated in anhydrous ethanol and made transparent with xylene. The transparent sections were sealed with drops of treacle. Histomorphology was observed and photographed under a light microscope.

Western blot analysis

The rest pulmonary lobe tissues were placed in refrigerator at -20°C for 6 h, and then stored in refrigerator at -80°C for later use. Protein extraction from lung tissues and A549 cells was carried out by employing a commercial radio immunoprecipitation assay (RIPA) lysis buffer (Elabscience Biotechnology Inc.). Protein concentration was determined by bicinchoninic acid (BCA) assay (Beijing Solarbio Science & Technology Co. Ltd.). After electrophoretic separation in 15% sodium dodecyl sulfate-polyacrylamide gel electrophoresis (SDS-PAGE), the protein samples (30 μg) were transferred to polyvinylidene fluoride (PVDF) membranes and subsequently blocked with 5% skimmed milk for 1 h. The blocked membranes were then subjected to incubation overnight at 4°C with primary antibodies against SIRT3 (1:1000; ab189860; Abcam), Bcl-2 (1:1000; ab32124; Abcam), Bax (1:1000; ab32503; Abcam), cleaved caspase3 (1:500; ab32042; Abcam), caspase3 (1:1000; ab184787; Abcam), cleaved poly(ADP-ribose) polymerase (PARP) (1:1000; ab32064; Abcam), FOXO1 (1:1000; ab179450; Abcam), FOXO1-acetylation (FOXO1-Ac, 1:2000; AF2305; Affinity Biosciences), and glyceraldehyde 3-phosphate dehydrogenase (GAPDH; 1:5000; ab201822; Abcam). Following a 10-min washing with tris buffered saline with tween (TBS-tween) 20 for three times, the membranes were incubated with a horseradish peroxidase-labeled goat anti-rabbit immunoglobulin G (IgG) secondary antibody (1:2000; ab6721; Abcam) for 1 h. GAPDH served as an internal reference. Protein bands were observed with enhanced ECL chemiluminescent substrate kit (Yeasen Biotechnology Co. Ltd., Shanghai, China), and the images were quantified with the ChemiDoc imaging system (Bio-Rad Laboratories Inc.).

Reverse transcription-quantitative polymerase chain reaction (RT-qPCR) assay

Total RNA was extracted from pulmonary lobe tissues and A549 cells with the total RNA extraction kit (Beijing Solarbio Science & Technology Co. Ltd.; Cat. No. R1200) according to the manufacturer's instructions. First strand complementary DNA (cDNA) synthesis was obtained from 1- μg RNA by using ImProm-ITM reverse transcription system (Promega Corporation). qPCR reaction was performed with SYBR Green Realtime PCR Master Max (Cat. No. QPK-201; Toyobo Life Science) on an ABI PRISM 7000 sequence detection system (Shanghai PuDi Biotech Co. Ltd.). The thermocycling conditions for PCR were as follows: at 95°C for 60 s and 95°C for 15 s, followed by an annealing

temperature of 60°C for 15 s, for a total of 40 cycles, and an extension temperature of 72°C for 45 s. GAPDH served as an internal reference. The relative messenger RNA (mRNA) expressions of *SIRT3*, *FOXO1*, *TNF- α* , *IL-1 β* , and *IL-6* genes were evaluated by the $2^{-\Delta\Delta\text{Ct}}$ method.²⁷ Sequences of the primers are shown in Tables 1 and 2.

Measurement of superoxide dismutase (SOD) and malondialdehyde (MDA)

In order to detect oxidative stress levels, the levels of SOD and MDA were detected by using the corresponding commercial enzyme-linked-immunosorbent serologic assay (ELISA) kits for SOD (Cat. No. S0086) and MDA (Cat. No. S0131S) (all obtained from Beyotime Institute of Biotechnology) according to the manufacturer's instructions.

Reactive oxygen species (ROS) assay

Reactive oxygen species levels in cells were detected using the fluorescent probe 2',7'-dichlorodihydrofluorescein (DCFH; Sigma-Aldrich; Merck KGaA), which was rapidly oxidized into a highly fluorescent 2',7'-dichlorofluorescein (DCF) in the presence of intracellular ROS. Then three fields were selected to detect fluorescence using a laser scanning confocal microscope (magnification, $\times 200$; Leica

Table 1 Target sequences for FOXO1 siRNAs.

Group	Target sequences (5'-3')
siFOXO1-1	CAATTCGTCATAATCTGTCCCTACA
siFOXO1-2	CAGAACGTCATGATGGGCCCTAATT
siRNA-NC	UAGCGACUAAACACAUCAA

Table 2 Primers for RT-qPCR analyses.

Primers	Sequence (5'-3')
Human SIRT3	F: ACCCAGTGGCATTCCAGAC R: GGCTTGGGGTTGTGAAAGAAG
Rat SIRT3	F: GGGTCCTTTGCTCTGAGTCC R: GGTAAGGTCCCTGGTCAGC
Human FOXO1	F: TCGTCATAATCTGTCCCTACACA R: CGGCTTCGGCTCTTAGCAAA
Rat FOXO1	F: GAGCAGTCCAAAGATGCCCT R: CAGAGCACAGGCAGTACACA
Human TNF- α	F: CTGGGCAGGTCTACTTTGGG R: CTGGAGGCCCCAGTTTGAAT
Human IL-1 β	F: GCTCGCCAGTGAAATGATGG R: TCGTGCACATAAGCCTCGTT
Human IL-6	F: CCACCGGAACGAAAGAGAA R: GAGAAGGCAACTGGACCGAA
Human GAPDH	F: AATGGGCAGCCGTTAGGAAA R: GCGCCCAATACGACCAATC
Rat GAPDH	F: GCATCTTCTTGTGCAGTGCC R: GATGGTGATGGGTTTCCCGT

Microsystems GmbH) at 488 nm. The ROS level was quantified as the relative fluorescence intensity of DCF per cell in the scan area using the ImageJ software version 1.4.6 (National Institutes of Health).

Cell apoptosis assay

The terminal deoxynucleotidyl transferase dUTP nickend labeling (TUNEL) staining method was used to detect apoptosis in A549 cells. Briefly, cells were cultured in 6-well plates for 24 h. Subsequently, the cells were fixed in 4% paraformaldehyde for 1 h at 25°C and then permeabilized with 0.1% Triton X-100 at 8°C for 15 min. Next, the cells were stained for 1 h at 37°C using 50- μ L *in situ* cell death detection kit (TUNEL reaction mix; Roche Applied Science). The cell nuclei were stained with 4',6-diamidino-2-phenylindole (DAPI) staining solution for 15 min at room temperature. Finally, 10 randomly selected areas in each section were evaluated under a fluorescence microscope (20X; Leica Microsystems GmbH), and the percentage of positive cells with green fluorescence was calculated with the ImageJ software, version 1.4.6 (National Institutes of Health). The percentage of apoptotic cells was determined by counting the TUNEL-positive cells and dividing the number by the total number of cells.

Statistical analysis

Experimental data are shown as mean \pm standard deviation (SD). All experiments were performed in triplicate. Differences in measured variables between two groups were evaluated using unpaired Student's *t*-test. One-way ANOVA was used for evaluation of differences between multiple groups, followed by Tukey's *post hoc* test. All analyses were performed using GraphPad Prism 5.0 (GraphPad Software Inc.). $P < 0.05$ was considered as statistically significant.

Results

SIRT3 expression is decreased in hyperoxia-induced tissues and cells

The H&E staining results revealed that hyperoxia induced structural disturbances in the lung tissues, with a marked increase in the volume of the alveolar cavity and a marked thickening of the septa (Figure 1A), which indicated that the hyperoxia-induced model was successfully established. SIRT3 expression was clearly downregulated in the hyperoxia-induced model group, compared to that of the control group (Figures 1B and 1C). Since SIRT3 is a mitochondrial protein, the present study also examined the levels of mitochondrial oxidative stress-related markers. The expression levels of SOD were markedly decreased, and that of MDA were increased in hyperoxia-induced lung tissues (Figures 1D and 1E). In addition, SIRT3 was also notably reduced in hyperoxia-induced A549 cells, compared to the control group (Figures 1F and 1G). Taken together, these results suggested that SIRT3 expression was downregulated in hyperoxia-induced lung tissues and A549 cells.

Overexpression of SIRT3 improves the hyperoxia-induced inflammatory response in A549 cells

In order to investigate whether SIRT3 expression has an effect on hyperoxia-induced inflammation in A549 cells, SIRT3 expression was detected in A549 cells. In A549 cells, the expression of SIRT3 was increased after plasmid transfection (Figures 2A and 2B). SIRT3 expression declined rapidly in hyperoxia-induced A549 cells, compared to that of the control group but increased in hyperoxia-induced A549 cells upon transfection of OV-SIRT3 (vs OV-NC; Figures 2C and 2D). The subsequent RT-qPCR assay indicated that the levels of TNF- α , IL-1 β , and IL-6 increased, compared to those in the control group, while OV-SIRT3 reduced the levels of inflammatory cytokines TNF- α , IL-1 β , and IL-6 in hyperoxia-induced A549 cells (vs OV-NC; Figure 2E). Taken together, these findings indicated that overexpression of SIRT3 markedly reduced hyperoxia-induced release of inflammatory factor in A549 cells.

Overexpression of SIRT3 alleviates hyperoxia-induced oxidative stress in A549 cells

A number of experiments were conducted to explore the effect of SIRT3 overexpression on hyperoxia-induced oxidative stress in A549 cells. Figure 3A shows that the ROS level increased in hyperoxia-induced A549 cells and it rapidly decreased upon transfection of OV-SIRT3. In contrast to the trend in ROS levels, Figure 3B reveals that the level of SOD declined markedly in the hyperoxia group, while it increased in the hyperoxia (6 h)+OV-SIRT3 group. In contrast, trend in the MDA level of each group was opposite to that of SOD. These results demonstrated that overexpression of SIRT3 alleviated oxidative stress induced by hyperoxia in A549 cells.

Overexpression of SIRT3 improves hyperoxia-induced apoptosis in A549 cells

Figure 4A shows more TUNEL-positive A549 cells in the hyperoxia group (vs the control group) and noticeably less TUNEL-positive cells in the hyperoxia (6 h)+OV-SIRT3 group (vs hyperoxia (6 h)+OV-NC group). Accordingly, hyperoxia induced a high apoptosis rate of ~35%, while SIRT2 overexpression reduced it to 15%. In addition, an increase in the levels of pro-apoptotic Bax, cleaved caspase3, and cleaved PARP was observed. A decrease in the levels of anti-apoptotic Bcl-2 in the hyperoxia group (vs. the control group), as well as reduced expression levels of Bax, cleaved caspase3, and cleaved PARP, and increased expression level of Bcl-2 in the hyperoxia (6 h)+OV-SIRT3 group (Figure 4B), was also observed. Taken together, these findings suggested that SIRT3 upregulation could inhibit hyperoxia-induced A549 cell apoptosis.

FOXO1 expression is reduced in hyperoxia-induced tissues and in A549 cells with elevated levels of FOXO1 acetylation

Western blot analysis displayed elevated FOXO1-Ac expression and decreased FOXO1 expression in the hyperoxia

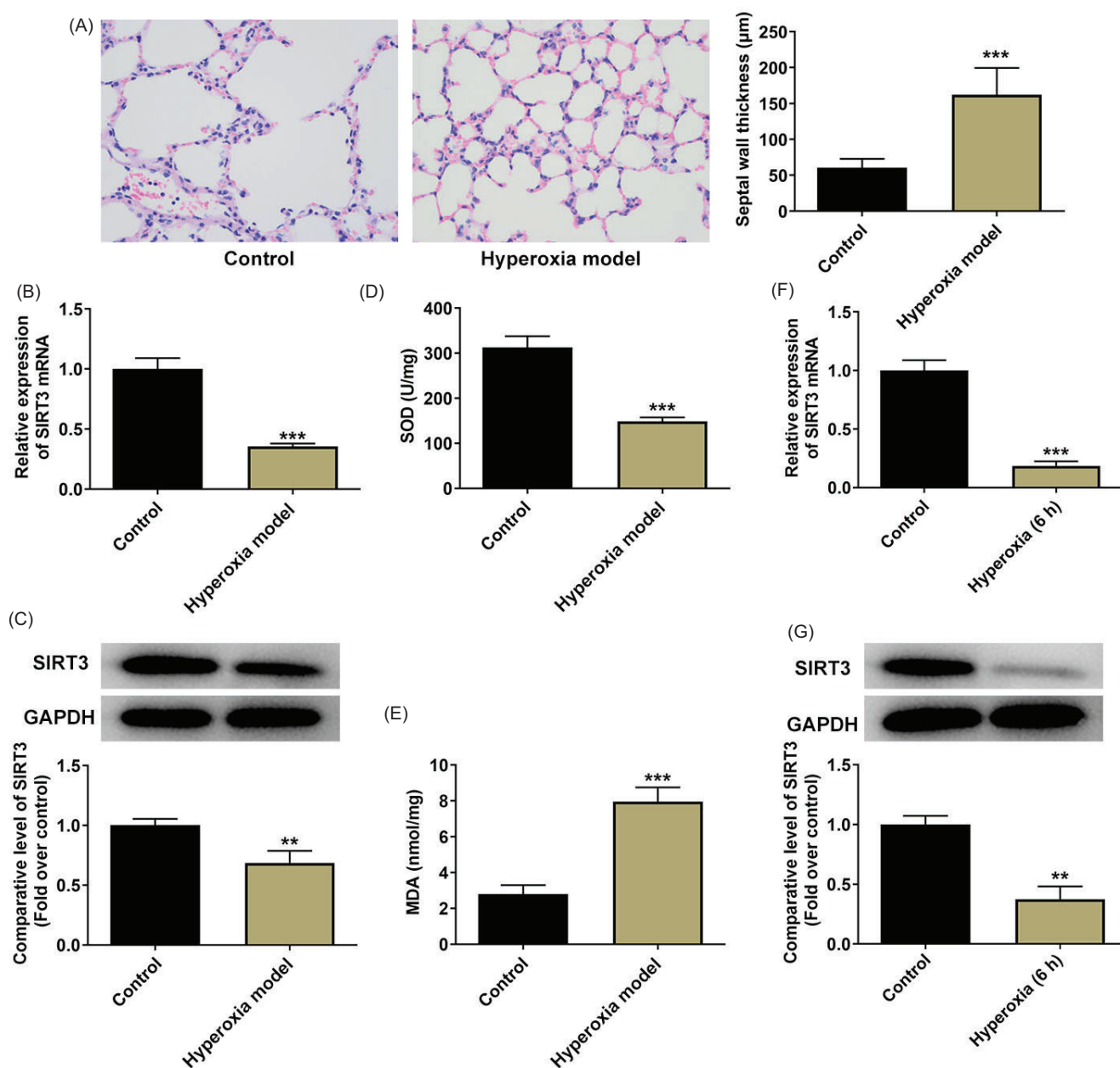


Figure 1 SIRT3 expression is decreased in hyperoxia-induced tissues and cells. (A) The pathological changes in hyperoxia-induced lung tissues were detected by H&E staining ($n = 3$). (B and C) SIRT3 expression was determined in hyperoxia-induced lung tissues with the application of RT-qPCR ($n = 5$) and Western blot analysis ($n = 3$). The levels of SOD(D) and MDA(E) in hyperoxia-induced lung tissues were assayed by corresponding kits ($n = 5$). (F and G) SIRT3 expression was determined in hyperoxia-induced A549 cells with the application of RT-qPCR ($n = 5$) and Western blot analysis ($n = 3$). $^{**}P < 0.01$, $^{***}P < 0.001$ vs control. GAPDH served as an internal reference in RT-qPCR. (A-G): Unpaired t -test with Tukey's *post hoc* test.

group, compared to that of the control group (Figure 5A). Similarly, an increase in the expression of FOXO1-Ac and a decrease in the expression of FOXO1 in hyperoxia-induced A549 cells were also observed (Figure 5B). Overall, these results showed that FOXO1 expression was decreased, while its acetylation level was increased in hyperoxia-induced tissues and cells.

Overexpression of SIRT3 inhibits the acetylation level of FOXO1 and activates FOXO1 expression in A549 cells

Whether SIRT3 overexpression also affected FOXO1 expression, was next evaluated. Figure 6 revealed that OV-SIRT3 markedly decreased the expression of FOXO1-Ac but

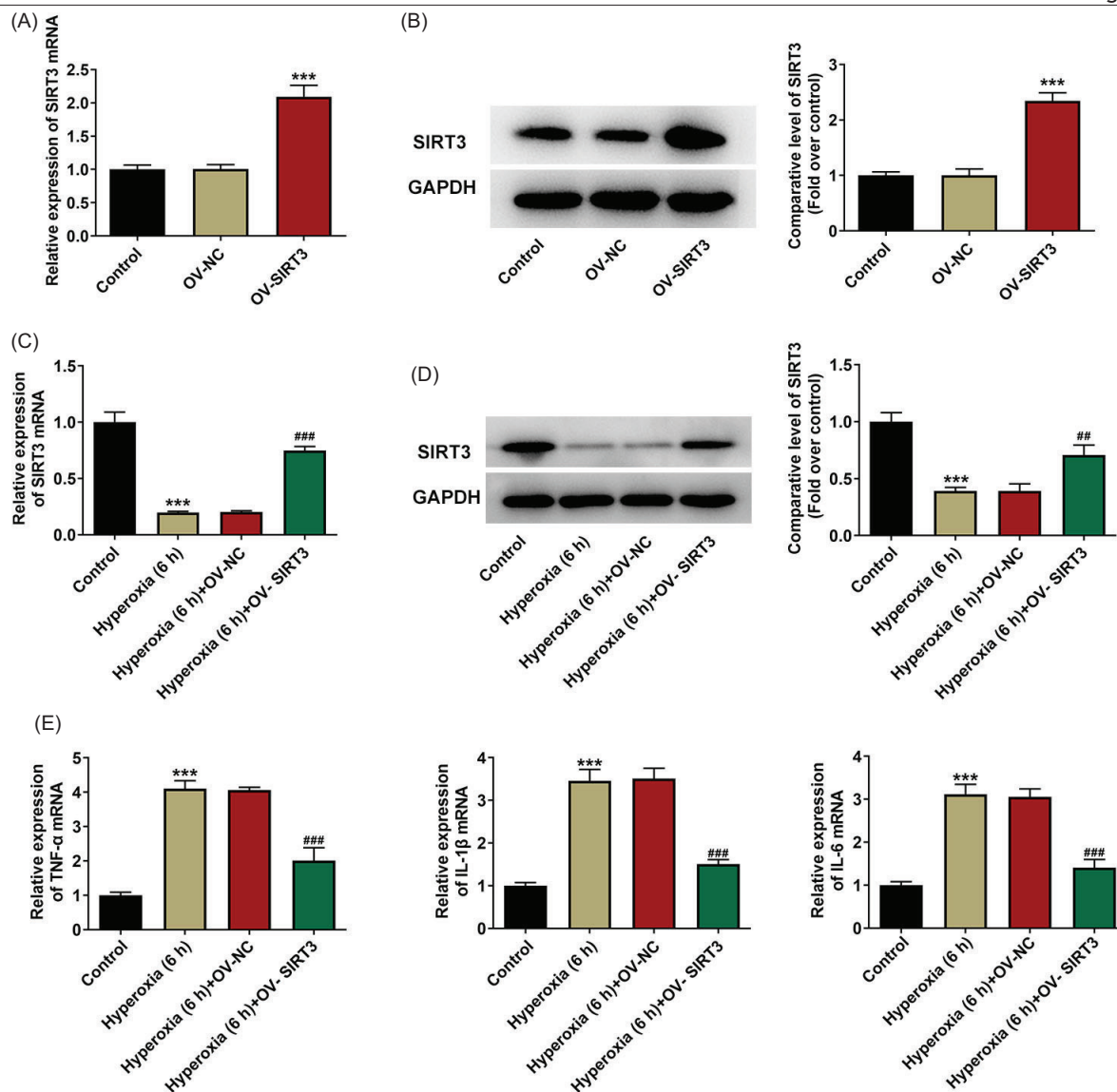


Figure 2 Overexpression of SIRT3 improves hyperoxia-induced inflammatory response in A549 cells. (A and B) The overexpression efficiency of SIRT3 expression was determined in A549 cells with the adoption of RT-qPCR ($n = 5$) and Western blot analysis ($n = 3$). (C and D) The overexpression efficiency of SIRT3 expression was determined in hyperoxia-induced A549 cells with the adoption of RT-qPCR ($n = 5$) and Western blot analysis ($n = 3$). (E) Levels of TNF- α , IL-1 β , and IL-6 were detected in hyperoxia-induced A549 cells employing RT-qPCR ($n = 5$). *** $P < 0.001$ vs control; ## $P < 0.01$, ### $P < 0.001$ vs hyperoxia (6 h)+OV-NC. GAPDH served as an internal reference in RT-qPCR. (A-E): One-way ANOVA with Tukey's multiple comparison test.

notably increased the expression of FOXO1 (vs the control group; Figure 6). These results indicated that SIRT3 overexpression could inhibit the acetylation level of FOXO1 and activate FOXO1 expression in A549 cells.

FOXO1 knockdown reverses the inhibitory role of SIRT3 overexpression in hyperoxia-induced inflammation and oxidative stress in A549 cells

Verification of the knockdown efficacy of siRNA-FOXO1-1/2 by RT-qPCR and Western blot analysis revealed that A549 cells transfected with siRNA-FOXO1-1 showed lower expression of FOXO1 than cells transfected with siRNA-FOXO1-2 (Figures 7A and 7B). Therefore, siRNA-FOXO1-1 plasmid

was selected for subsequent experiments. As aforementioned, SIRT3 overexpression could suppress the levels of TNF- α , IL-1 β , and IL-6 and oxidative stress in A549 cells. However, co-transfection of OV-SIRT3 and siRNA-FOXO1 increased the expression levels of TNF- α , IL-1 β , and IL-6 (vs siRNA-NC; Figure 7C). Furthermore, levels of TNF- α , IL-1 β , and IL-6 were increased in the hyperoxia (6 h)+OV-SIRT3+siRNA-FOXO1 group, in comparison to those in the hyperoxia (6 h)+OV-SIRT3+siRNA-NC group (Figure 7D). ROS levels in the OV-SIRT3 group decreased, compared to the OV-NC group and increased in the OV-SIRT3+siRNA-FOXO1 group, compared to OV-SIRT3+siRNA-NC group (Figure 7E). Furthermore, ROS levels were increased in the hyperoxia (6 h)+OV-SIRT3+siRNA-FOXO1 group, in comparison to those in the hyperoxia (6 h)+OV-SIRT3+siRNA-NC group (Figure 7F).

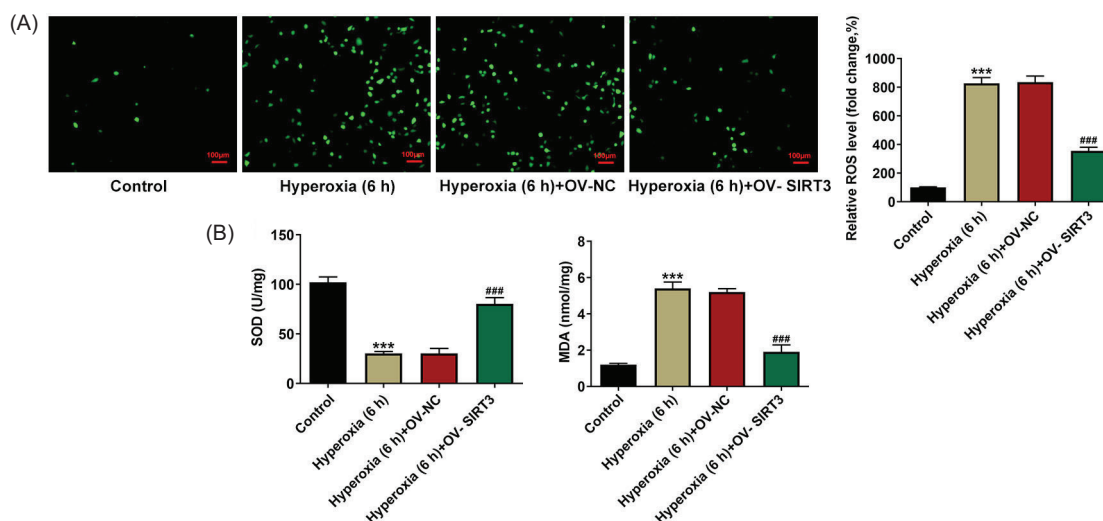


Figure 3 Overexpression of SIRT3 alleviates hyperoxia-induced oxidative stress in A549 cells. (A) ROS level was assessed in hyperoxia-induced A549 cells by means of ROS assay kit ($n = 3$). Green fluorescence represents ROS expression. (B) Content of SOD and MDA was detected in hyperoxia-induced A549 cells by using SOD and MDA assay kits ($n = 5$). *** $P < 0.001$ vs control; ### $P < 0.001$ vs hyperoxia (6 h)+OV-NC. (A and B): One-way ANOVA with Tukey's multiple comparison test.

Consistently, decreased SOD levels and increased MDA levels were observed in the OV-SIRT3+siRNA-FOXO1 group, compared to the OV-SIRT3+siRNA-NC group, and in the hyperoxia (6 h)+OV-SIRT3+siRNA-FOXO1 group, compared to hyperoxia (6 h)+OV-SIRT3+siRNA-NC group (Figures 7G and 7H). These results indicated that knockdown of FOXO1 could diminish the suppressive role of SIRT3 upregulation in the inflammation and oxidative stress of A549 cells subjected to hyperoxia induction.

FOXO1 knockdown reverses the suppressive role of SIRT3 overexpression in hyperoxia-induced apoptosis in A549 cells

Figure 8A shows that hyperoxia-induced A549 cells co-transfected with OV-SIRT3, and siRNA-FOXO1 showed a higher apoptosis rate, compared to that of the cells transfected only with OV-SIRT3 under hyperoxia induction. In addition, levels of Bax, cleaved caspase3, and cleaved PARP increased whereas that of Bcl-2 decreased in the hyperoxia (6 h)+OV-SIRT3+siRNA-FOXO1 group, compared to those in the hyperoxia (6 h)+OV-SIRT3+siRNA-NC group (Figure 8B). These findings suggested that knockdown of FOXO1 could reverse the inhibitory role of SIRT3 overexpression in hyperoxia-induced A549 cell apoptosis.

Discussion

Bronchopulmonary dysplasia is the most common pulmonary complication diagnosed in preterm infants, and is closely associated with hyperoxia.²⁸ Previous data have suggested that inflammation, oxidative stress, and apoptosis are key pathogenic mechanisms in BPD.²⁹ Extensive investigative studies have demonstrated the role of

SIRT3 as a mitochondrial deacetylase in the regulation of mitochondrial DNA damage in both AECs and lung diseases.³⁰⁻³² Therefore, the present study explored the function of SIRT3 in BPD, and found that SIRT3 was lowly expressed in hyperoxia-induced lung tissues and A549 cells. Overexpression of SIRT3 improved hyperoxia-induced inflammation, oxidative stress, and apoptosis. In addition, SIRT3 overexpression also inhibited the acetylation level of FOXO1 and activated FOXO1 expression. However, knockdown of FOXO1 reversed the effect of SIRT3 overexpression on hyperoxia-induced A549 cells.

Hyperoxia therapy is employed to improve respiratory distress in neonates, children, and adults.¹⁶ However, high concentrations of oxygen produce a large number of toxic products, such as ROS, hydrogen peroxide, and free radicals in the body, and premature infants are not able to remove these toxic products in time.³³ ROS metabolites play a vital role in the pathogenesis of BPD, which interfere with cell metabolism and inhibit the synthesis of protease and DNA, resulting in extensive cell and tissue damage.³⁴ In addition, high concentrations of oxygen cause nonspecific changes, such as pulmonary edema, inflammatory fibrin deposition, and decreased lung surface activity.³⁵ A549 cells are not only cancer cells but also a type of lung epithelial cells that can be used to study BPD.^{24,36,37}

Therefore, the present study used a concentration of 90% O₂ to induce neonatal rats and A549 cells to establish animal model and cell models of BPD, respectively. After 14 days of induction with 90% O₂, the alveolar wall was thickened in lung tissues, indicating that the BPD model was successfully established. It was previously found that SIRT3 expression was reduced in hyperoxia-induced lung tissues and A549 cells.³⁸ The present study found that SIRT3 was similarly downregulated in a significant manner in hyperoxia-induced lung tissues and A549 cells, suggesting that aberrant SIRT3 expression was closely associated with BPD.

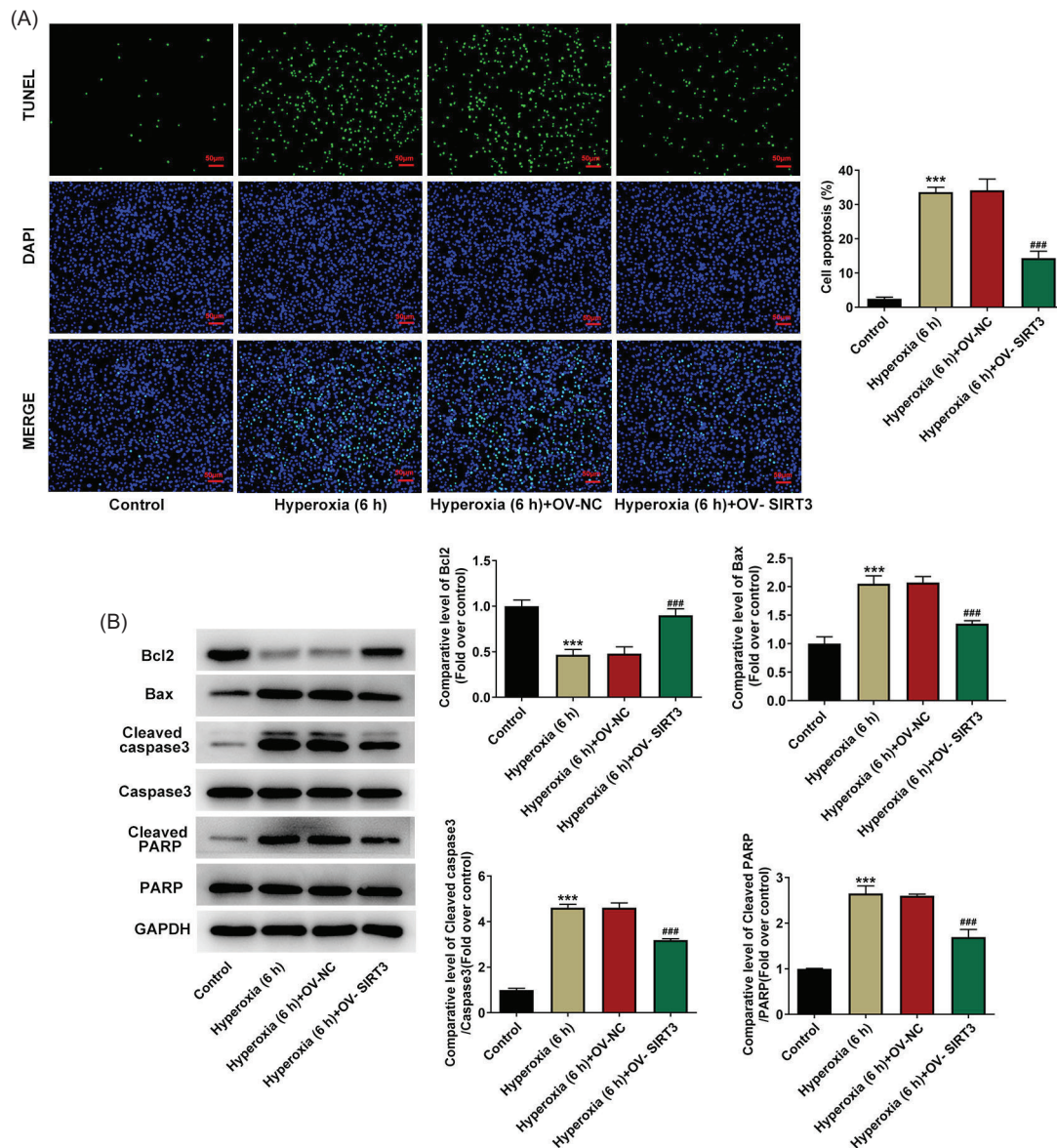


Figure 4 Overexpression of SIRT3 improves hyperoxia-induced apoptosis in A549 cells. (A) Cell apoptosis in hyperoxia-induced A549 cells was assessed by using TUNEL staining ($n = 3$). (B) Levels of apoptosis-related factors Bax, cleaved caspase3, cleaved PARP, and Bcl-2 were detected by Western blot analysis ($n = 3$). *** $P < 0.001$ vs control; ### $P < 0.001$ vs hyperoxia (6 h)+OV-NC. (A and B): One-way ANOVA with Tukey's multiple comparison test.

Inflammation has been a key part of BPD pathogenesis,¹³ since hyperoxia induces excessive generation of ROS, thus causing lung epithelial cell damage, increasing lung permeability, and activating the release of inflammatory factors.³⁹ This was also confirmed by the increased levels of IL-1 β , IL-6, and TNF- α found in the tracheal aspirates of BPD patients.⁴⁰

SIRT3 has been reported to have anti-inflammatory effects in a variety of diseases. For instance, SIRT3 overexpression inhibits TNF- α -induced inflammation in human and neonatal rat cardiomyocytes.⁴¹ SIRT3 inhibits macrophage-mediated inflammation in wound repair.⁴² Activation of SIRT3 also suppresses inflammatory response and reduces lung injury.⁹ Therefore, an overexpression plasmid of SIRT3 was constructed in the present study. It was

observed that the elevated levels of pro-inflammatory factors induced by hyperoxia were significantly reduced upon SIRT3 overexpression, suggesting that overexpression of SIRT3 improved the inflammatory response of A549 cells.

Increasing evidence is discovered that oxidative stress plays an important role in the development of BPD⁴³ by targeting immature AECs exposed to high oxygen levels.¹ A previous study has also reported that oxidative stress-mediated apoptosis of AECs is involved in hyperoxia-induced lung injury in neonatal rats,⁴⁴ since oxidative stress causes overproduction of ROS in cells and damages mitochondrial proteins, lipids, and mitochondrial DNA.⁴⁵ SIRT3 is a regulator of antioxidant response and mitochondrial homeostasis.⁴⁶ It has been reported that SIRT3 indirectly reduces the

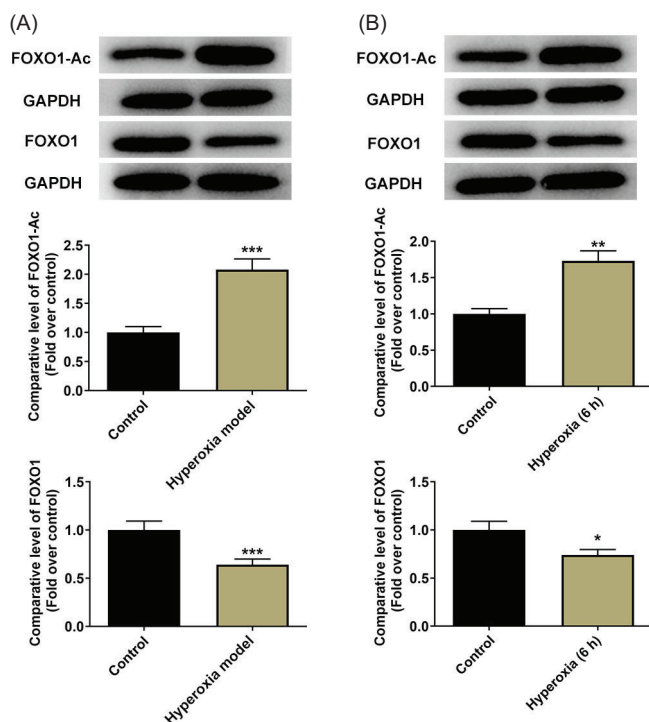


Figure 5 FOXO1 expression is reduced in hyperoxia-induced tissues and cells with elevated levels of its acetylation in A549 cells. (A) The acetylation level and overall expression of FOXO1 in hyperoxia-induced lung tissues was determined by Western blot analysis ($n = 3$). (B) The acetylation level and overall expression of FOXO1 in hyperoxia-induced A549 cells was determined by Western blot analysis ($n = 3$). * $P < 0.05$, ** $P < 0.01$, *** $P < 0.001$ vs control. (A and B): Unpaired t -test with Tukey's *post hoc* test.

generation of ROS by promoting electron transport through deacetylation of electron transport chain complex.⁴⁷ SIRT3 also prevents pulmonary fibrosis by inhibiting mitochondrial DNA damage and apoptosis in AECs.¹²

These findings indicate the inhibitory effect of SIRT3 on oxidative stress. Furthermore, overexpression of SIRT3

significantly reduces ROS levels in A549 cells through upregulation of P53 and P21 protein levels.⁴⁸ Similarly, the present study also found that SIRT3 overexpression significantly reduced ROS and MDA levels, and increased SOD levels, suggesting that the upregulation of SIRT3 could alleviate oxidative stress caused by high oxygen levels.

It has been suggested that the apoptosis of AECs is an important feature of hyperoxia-induced lung injury,⁴⁹ since hyperoxia-induced AECs may increase Bax level in mitochondrial membrane, which in turn leads to apoptosis.⁵⁰ SIRT3 has been found to function through several anti-apoptotic pathways. SIRT3 inhibits apoptosis by closing mitochondrial permeability transition pore to maintain the normal morphology of mitochondria.⁵¹ Upregulation of SIRT3 can also inhibit apoptosis by regulating the Akt signaling pathway.⁵² The Bcl-2 family of proteins is important for activating different caspases in mitochondria and regulating cell apoptosis.⁵³ It has been reported that overexpression of SIRT3 in A549 cells induces apoptosis and increases Bax-Bcl-2 and Bax-Bcl-xl ratios.⁴⁸ The present study exhibited reduced apoptotic cell rates and reduced levels of pro-inflammatory cytokines Bax, cleaved caspase3, and cleaved PARP, and elevated Bcl-2 expression.

These results confirmed the inhibitory effect of SIRT3 overexpression on the hyperoxia-induced apoptosis of A549 cells. FOXO1, a transcription factor belonging to the FOXO protein family, has been reported to exhibit reduced expression in a hyperoxia-induced acute lung injury mouse model.²⁰ The present study found that FOXO1 expression was decreased in both hyperoxia-induced lung tissues and cells, but its acetylation levels were elevated. The transcriptional activity of FOXO1 is regulated by post-translational modifications, such as phosphorylation, acetylation, and ubiquitination.⁵⁴ SIRT3 is a mitochondrial protein deacetylase.⁸ Its overexpression upregulates FOXO1 expression through its deacetylase activity.⁵⁵ This was consistent with increase in FOXO1 and decrease in FOXO1-AC following SIRT3 overexpression in the present study. It has been suggested that CD28 knockout helps to alleviate lung inflammation, oxidative stress, apoptosis, and T-cell aggregation induced by blast exposure through PI3K-Akt-FOXO1 signaling.⁵⁶ Furthermore, microRNA-486 protects A549 cells from PM2.5-induced

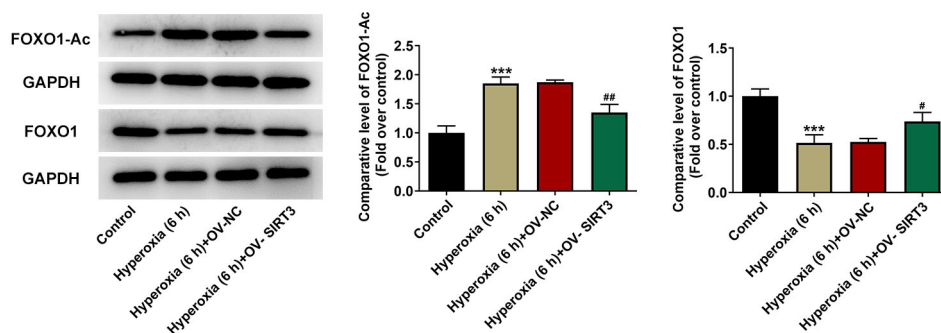


Figure 6 Overexpression of SIRT3 inhibits the acetylation level of FOXO1 and activates FOXO1 expression in A549 cells. The acetylation level and overall expression of FOXO1 in hyperoxia-induced A549 cells transfected with OV-SIRT3 was determined by Western blot analysis ($n = 3$). *** $P < 0.001$ vs control; # $P < 0.05$, ## $P < 0.01$ vs hyperoxia (6 h)+OV-NC. One-way ANOVA with Tukey's multiple comparison test.

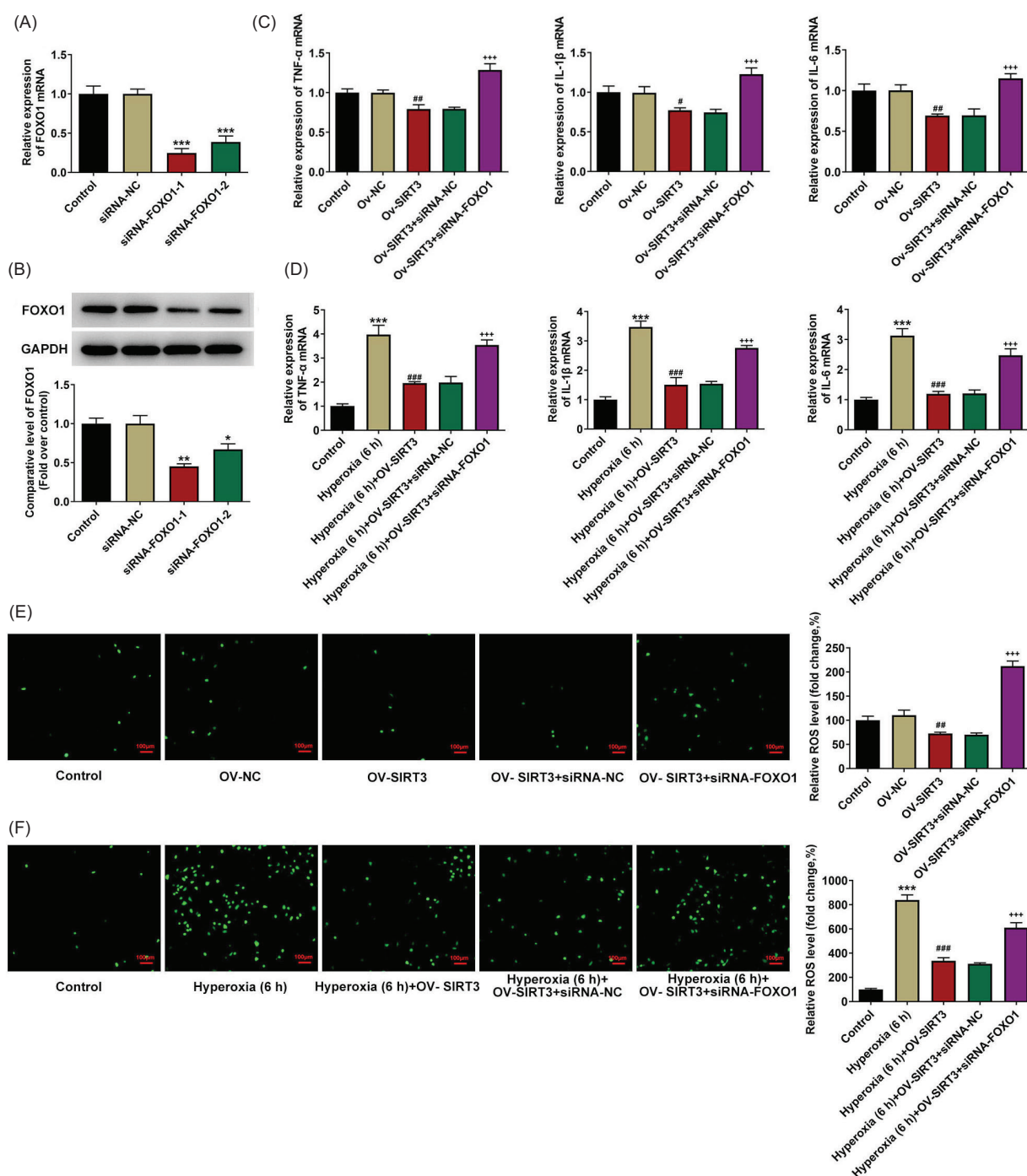


Figure 7 FOXO1 knockdown reverses the inhibitory role of SIRT3 overexpression of hyperoxia-induced inflammation and oxidative stress in A549 cells. (A and B) Expression of FOXO1 in A549 cells transfected with siRNA-FOXO1-1/2 was examined by using RT-qPCR ($n = 5$) and Western blot analysis ($n = 3$). * $P < 0.05$, ** $P < 0.01$, *** $P < 0.001$ vs siRNA-NC. (C) Levels of TNF- α , IL-1 β , and IL-6 were detected in A549 cells co-transfected with OV-SIRT3 and siRNA-FOXO1 employing RT-qPCR ($n = 5$). (D) Levels of TNF- α , IL-1 β , and IL-6 were detected in hyperoxia-induced A549 cells co-transfected with OV-SIRT3 and siRNA-FOXO1 employing RT-qPCR ($n = 5$). (E) ROS level was assessed in A549 cells co-transfected with OV-SIRT3 and siRNA-FOXO1 by means of ROS assay kit ($n = 3$). Green fluorescence represents ROS expression. (F) ROS level was assessed in hyperoxia-induced A549 cells co-transfected with OV-SIRT3 and siRNA-FOXO1 by means of ROS assay kit ($n = 3$). Green fluorescence represents ROS expression.

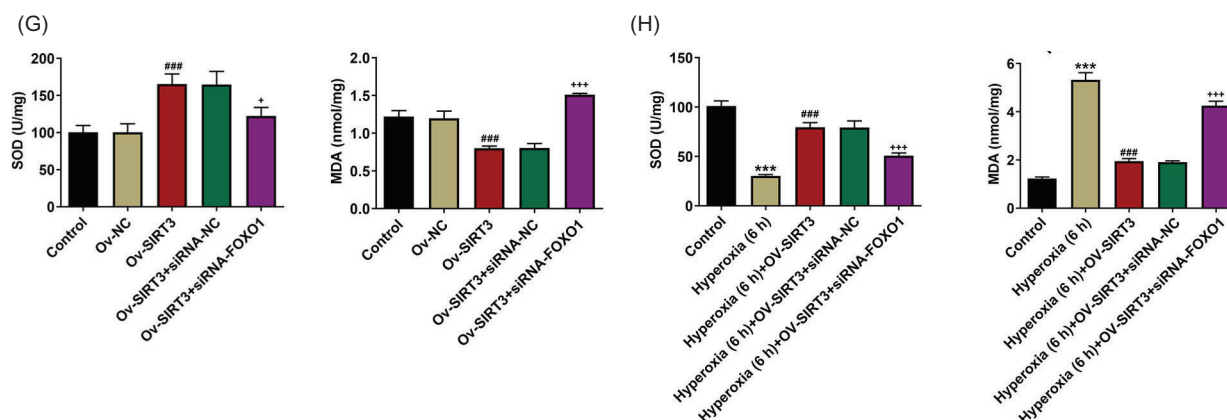


Figure 7 (Continued). (G) Content of SOD and MDA was detected in A549 cells co-transfected with OV-SIRT3 and siRNA-FOXO1 by using SOD and MDA assay kits ($n = 5$). (H) Content of SOD and MDA was detected in hyperoxia-induced A549 cells co-transfected with OV-SIRT3 and siRNA-FOXO1 by using SOD and MDA assay kits ($n = 5$). ^{***} $P < 0.001$ vs control; ^{###} $P < 0.001$ vs hyperoxia (6 h); ⁺⁺⁺ $P < 0.001$ vs hyperoxia (6 h)+OV-SIRT3+siRNA-NC. GAPDH served as an internal reference in RT-qPCR. (A-H): One-way ANOVA with Tukey's multiple comparison test.

cytotoxicity by targeting PTEN and FOXO1.²¹ FOXO1 knockdown may have the opposite effect. This was verified in the present study, which revealed that FOXO1 knockdown reversed the protective effect of SIRT3 overexpression on hyperoxia-induced A549 cells.

Limitations

There are several limitations to our study. First, we examined the expression of FOXO1, TNF- α , IL-1 β , and IL-6, as well as apoptosis-related indicators, in cell experiments only. Our study failed to examine these expressions in animals, which needs investigation in the future studies. Second, our research was carried out in A549 cells, which were also lung cancer cells having certain characteristics of lung cancer. The future investigations must choose other cell lines, such as primary lung epithelial cells, for further validation. In addition, concerning the induction time of hyperoxia, we only selected 6 h of induction. In the future experiments, hyperoxia induction must be conducted at different periods. Moreover, the present study failed to conduct investigations without hyperoxia, which must be analyzed in the future experiments.

Conclusions

Collectively, the present results suggested a critical role for SIRT3, and indicated that its protective effect on hyperoxia-induced BPD was achieved through deacetylation of FOXO1. These findings could provide certain insight into the molecular mechanism in BPD, and SIRT3 and FOXO1 could be used as molecular markers for the prevention or diagnosis of BPD. In addition, development of SIRT3- and

FOXO1-targeted drugs would be able to treat BPD effectively. Therefore, our study provides a theoretical basis for the clinical treatment of BPD.

Availability of data and materials

The datasets used and/or analyzed in the present study are available from the corresponding author on reasonable request.

Author contributions

Lili Zang and Jinghan Chi designed the experiments and made considerable contributions to write the manuscript. Lili Zang, Sitong Bi, and Lihua Li performed the experiments and analyzed the data. Jinghan Chi, Yi Tao, and Rong Wang revised the manuscript and guided the experiments. All authors confirmed the authenticity of the raw data, and read and approved the final manuscript.

Ethics approval and consent to participate

All animal experiments were in compliance with the Laboratory Animal Ethics Committee regulations of Beijing Luhe Hospital, and animal experiments were reported in accordance with the ARRIVE guidelines.

Competing interests

The authors stated that they had no competing interests to declare.

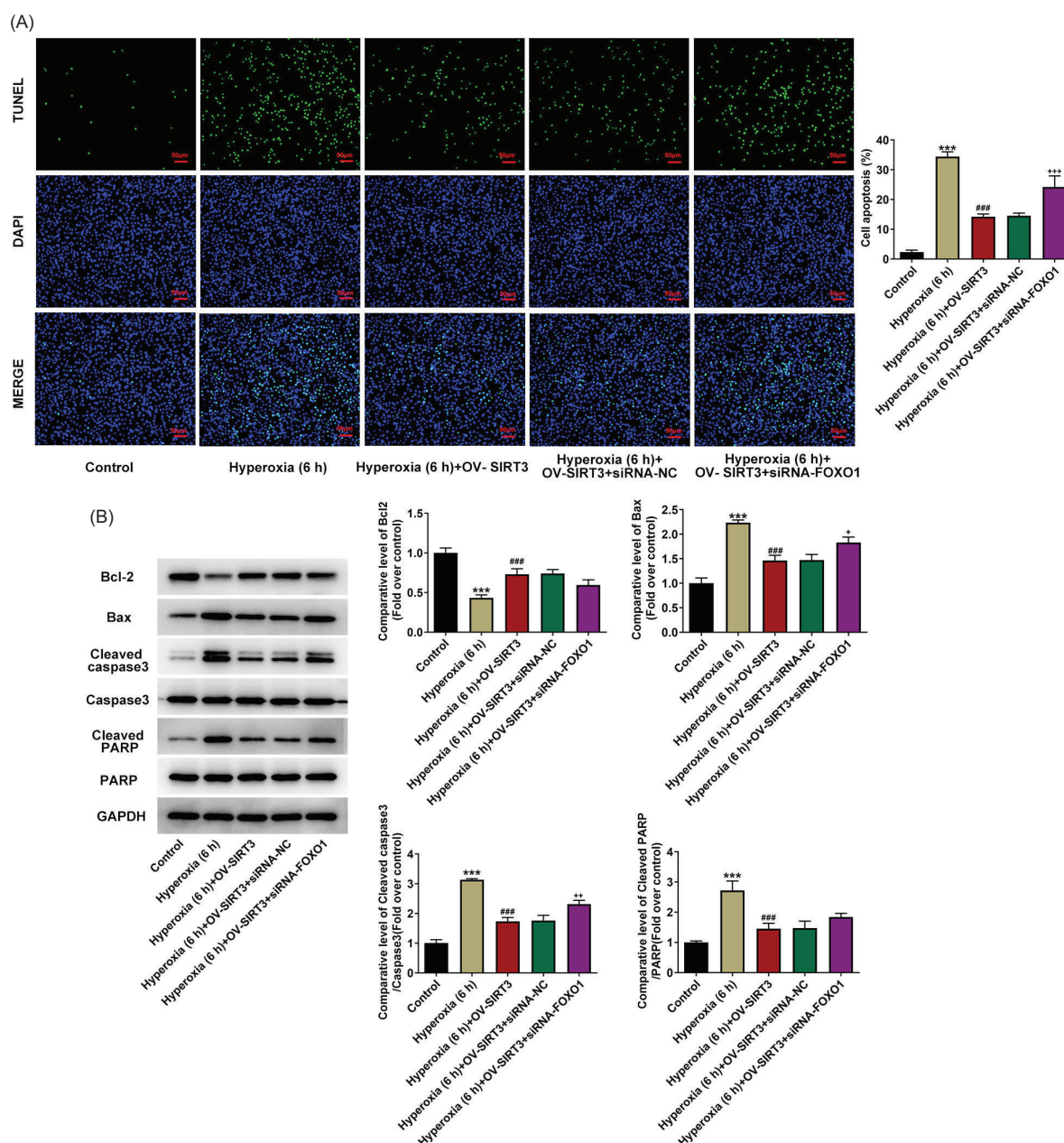


Figure 8 FOXO1 knockdown reverses the suppressive role of SIRT3 overexpression of hyperoxia-induced apoptosis in A549 cells. (A) Cell apoptosis in hyperoxia-induced A549 cells co-transfected with OV-SIRT3 and siRNA-FOXO1 was assessed making use of TUNEL staining ($n = 3$). (B) Levels of Bax, cleaved caspase3, cleaved PARP, and Bcl-2 were subjected to detection in hyperoxia-induced A549 cells co-transfected with OV-SIRT3 and siRNA-FOXO1 using Western blot analysis ($n = 3$). *** $P < 0.001$ vs control; ### $P < 0.001$ vs hyperoxia (6 h); * $P < 0.05$, ** $P < 0.01$ vs hyperoxia (6 h)+OV-SIRT3+siRNA-NC. (A-B): One-way ANOVA with Tukey's multiple comparison test.

References

- Zhu X, Wang F, Lei X, Dong W. Resveratrol alleviates alveolar epithelial cell injury induced by hyperoxia by reducing apoptosis and mitochondrial dysfunction. *Exp Biol Med* (Maywood). 2021;246:596-606. <https://doi.org/10.1177/1535370220975106>
- Principi N, Di Pietro GM, Esposito S. Bronchopulmonary dysplasia: Clinical aspects and preventive and therapeutic strategies. *J Transl Med*. 2018;16:36. <https://doi.org/10.1186/s12967-018-1417-7>
- Gauldie J, Galt T, Bonniaud P, Robbins C, Kelly M, Warburton D. Transfer of the active form of transforming growth factor-beta 1 gene to newborn rat lung induces changes consistent with bronchopulmonary dysplasia. *Am J Pathol*. 2003;163:2575-2584. [https://doi.org/10.1016/S0002-9440\(10\)63612-7](https://doi.org/10.1016/S0002-9440(10)63612-7)
- Reddy R, Buckley S, Doerken M, Barsky L, Weinberg K, Anderson KD, et al. Isolation of a putative progenitor subpopulation of alveolar epithelial type 2 cells. *Am J Physiol Lung Cell Mol Physiol*. 2004;286:L658-667. <https://doi.org/10.1152/ajplung.00159.2003>

5. Wang Y, Huang C, Reddy Chintagari N, Bhaskaran M, Weng T, Guo Y, et al. miR-375 regulates rat alveolar epithelial cell trans-differentiation by inhibiting Wnt/beta-catenin pathway. *Nucleic Acids Res.* 2013;41:3833-3844. <https://doi.org/10.1093/nar/gks1460>
6. Roper JM, Mazzatti DJ, Watkins RH, Maniscalco WM, Keng PC, O'Reilly MA. In vivo exposure to hyperoxia induces DNA damage in a population of alveolar type II epithelial cells. *Am J Physiol Lung Cell Mol Physiol.* 2004;286:L1045-54. <https://doi.org/10.1152/ajplung.00376.2003>
7. Wikenheiser KA, Wert SE, Wispe JR, Stahlman M, D'Amore-Bruno M, Singh G, et al. Distinct effects of oxygen on surfactant protein B expression in bronchiolar and alveolar epithelium. *Am J Physiol.* 1992;262:L32-39. <https://doi.org/10.1152/ajplung.1992.262.1.L32>
8. Kim TS, Jin YB, Kim YS, Kim S, Kim JK, Lee HM, et al. SIRT3 promotes antimicrobial defenses by coordinating mitochondrial and autophagic functions. *Autophagy.* 2019;15:1356-75. <https://doi.org/10.1080/15548627.2019.1582743>
9. Kurundkar D, Kurundkar AR, Bone NB, Becker Jr. EJ, Liu W, Chacko B, et al. SIRT3 diminishes inflammation and mitigates endotoxin-induced acute lung injury. *JCI Insight.* 2019;4(1):e120722. <https://doi.org/10.1172/jci.insight.120722>
10. Cheresh P, Kim SJ, Jablonski R, Watanabe S, Lu Z, Chi M, et al. SIRT3 overexpression ameliorates asbestos-induced pulmonary fibrosis, mt-DNA damage, and lung fibrogenic monocyte recruitment. *Int J Mol Sci.* 2021;22(13):6856. <https://doi.org/10.3390/ijms22136856>
11. Cao Y, Li P, Wang H, Li L, Li Q. SIRT3 promotion reduces resistance to cisplatin in lung cancer by modulating the FOXO3/CDT1 axis. *Cancer Med.* 2021;10:1394-404. <https://doi.org/10.1002/cam4.3728>
12. Jablonski RP, Kim SJ, Cheresh P, Williams DB, Morales-Nebreda L, Cheng Y, et al. SIRT3 deficiency promotes lung fibrosis by augmenting alveolar epithelial cell mitochondrial DNA damage and apoptosis. *FASEB J.* 2017;31:2520-32. <https://doi.org/10.1096/fj.201601077R>
13. Bhandari A, Bhandari V. Pathogenesis, pathology and pathophysiology of pulmonary sequelae of bronchopulmonary dysplasia in premature infants. *Front Biosci.* 2003;8:e370-80. <https://doi.org/10.2741/1060>
14. Chen Y, Chang L, Li W, Rong Z, Liu W, Shan R, et al. Thioredoxin protects fetal type II epithelial cells from hyperoxia-induced injury. *Pediatr Pulmonol.* 2010;45:1192-200. <https://doi.org/10.1002/ppul.21307>
15. McGrath-Morrow SA, Stahl J. Apoptosis in neonatal murine lung exposed to hyperoxia. *Am J Respir Cell Mol Biol.* 2001;25:150-55. <https://doi.org/10.1165/ajrcmb.25.2.4362>
16. O'Reilly MA, Staversky RJ, Finkelstein JN, Keng PC. Activation of the G2 cell cycle checkpoint enhances survival of epithelial cells exposed to hyperoxia. *Am J Physiol Lung Cell Mol Physiol.* 2003;284:L368-75. <https://doi.org/10.1152/ajplung.00299.2002>
17. Wang Y, Lyu Z, Qin Y, Wang X, Sun L, Zhang Y, et al. FOXO1 promotes tumor progression by increased M2 macrophage infiltration in esophageal squamous cell carcinoma. *Theranostics.* 2020;10:11535-48. <https://doi.org/10.7150/thno.45261>
18. Gao Z, Liu R, Ye N, Liu C, Li X, Guo X, et al. FOXO1 inhibits tumor cell migration via regulating cell surface morphology in non-small cell lung cancer cells. *Cell Physiol Biochem.* 2018;48:138-48. <https://doi.org/10.1159/000491670>
19. Sun K, Huang R, Yan L, Li DT, Liu YY, Wei XH, et al. Schisandrin attenuates lipopolysaccharide-induced lung injury by regulating TLR-4 and Akt/FoxO1 signaling pathways. *Front Physiol.* 2018;9:1104. <https://doi.org/10.3389/fphys.2018.01104>
20. Ruan Y, Dong W, Kang L, Lei X, Zhang R, Wang F, et al. The changes of Twist1 pathway in pulmonary microvascular permeability in a newborn rat model of hyperoxia-induced acute lung injury. *Front Pediatr.* 2020;8:190. <https://doi.org/10.3389/fped.2020.00190>
21. Li J, Zhou Q, Liang Y, Pan W, Bei Y, Zhang Y, et al. miR-486 inhibits PM2.5-induced apoptosis and oxidative stress in human lung alveolar epithelial A549 cells. *Ann Transl Med.* 2018;6:209. <https://doi.org/10.21037/atm.2018.06.09>
22. Xi J, Chen Y, Jing J, Zhang Y, Liang C, Hao Z, et al. Sirtuin 3 suppresses the formation of renal calcium oxalate crystals through promoting M2 polarization of macrophages. *J Cell Physiol.* 2019;234:11463-73. <https://doi.org/10.1002/jcp.27803>
23. Wang Y, Chen J, Kong W, Zhu R, Liang K, Kan Q, et al. Regulation of SIRT3/FOXO1 signaling pathway in rats with non-alcoholic steatohepatitis by salvianolic acid B. *Arch Med Res.* 2017;48:506-12. <https://doi.org/10.1016/j.arcmed.2017.11.016>
24. Li Z, Chen Y, Li W, Yan F. Cell division cycle 2 protects neonatal rats against hyperoxia-induced bronchopulmonary dysplasia. *Yonsei Med J.* 2020;61:679-88. <https://doi.org/10.3349/ymj.2020.61.8.679>
25. Danneman PJ, Mandrell TD. Evaluation of five agents/methods for anesthesia of neonatal rats. *Lab Anim Sci.* 1997;47:386-95.
26. Percie du Sert N, Ahluwalia A, Alam S, Avey MT, Baker M, Browne WJ, et al. Reporting animal research: Explanation and elaboration for the ARRIVE guidelines 2.0. *PLoS Biol.* 2020;18:e3000411. <https://doi.org/10.1371/journal.pbio.3000411>
27. Livak KJ, Schmittgen TD. Analysis of relative gene expression data using real-time quantitative PCR and the 2(-Delta Delta C(T)) method. *Methods.* 2001;25:402-8. <https://doi.org/10.1006/meth.2001.1262>
28. Ballabh P, Simm M, Kumari J, Krauss AN, Jain A, Califano C, et al. Neutrophil and monocyte adhesion molecules in bronchopulmonary dysplasia, and effects of corticosteroids. *Arch Dis Child Fetal Neonatal Ed.* 2004;89:F76-83. <https://doi.org/10.1136/fn.89.1.F76>
29. Kalikkot Thekkeveedu R, Guaman MC, Shivanna B. Bronchopulmonary dysplasia: A review of pathogenesis and pathophysiology. *Respir Med.* 2017;132:170-7. <https://doi.org/10.1016/j.rmed.2017.10.014>
30. Kim SJ, Cheresh P, Jablonski RP, Williams DB, Kamp DW. The role of mitochondrial DNA in mediating alveolar epithelial cell apoptosis and pulmonary fibrosis. *Int J Mol Sci.* 2015;16:21486-519. <https://doi.org/10.3390/ijms160921486>
31. Cao K, Chen Y, Zhao S, Huang Y, Liu T, Liu H, et al. Sirt3 promoted DNA damage repair and radioresistance through ATM-Chk2 in non-small cell lung cancer cells. *J Cancer.* 2021;12:5464-72. <https://doi.org/10.7150/jca.53173>
32. Bindu S, Pillai VB, Kanwal A, Samant S, Mutlu GM, Verdin E, et al. SIRT3 blocks myofibroblast differentiation and pulmonary fibrosis by preventing mitochondrial DNA damage. *Am J Physiol Lung Cell Mol Physiol.* 2017;312:L68-78. <https://doi.org/10.1152/ajplung.00188.2016>
33. Giusto K, Wanczyk H, Jensen T, Finck C. Hyperoxia-induced bronchopulmonary dysplasia: Better models for better therapies. *Dis Model Mech.* 2021;14(2):dmm047753. <https://doi.org/10.1242/dmm.047753>
34. Xuefei Y, Xinyi Z, Qing C, Dan Z, Ziyun L, Hejuan Z, et al. Effects of hyperoxia on mitochondrial homeostasis: Are mitochondria the hub for bronchopulmonary dysplasia? *Front Cell Dev Biol.* 2021;9:642717. <https://doi.org/10.3389/fcell.2021.642717>
35. Everitt LH, Awoseyila A, Bhatt JM, Johnson MJ, Vollmer B, Evans HJ. Weaning oxygen in infants with bronchopulmonary dysplasia. *Paediatr Respir Rev.* 2021;39:82-9. <https://doi.org/10.1016/j.prrv.2020.10.005>

36. Zhang M, Zhang X, Chu X, Cheng L, Cai C. Long non-coding RNA MALAT1 plays a protective role in bronchopulmonary dysplasia via the inhibition of apoptosis and interaction with the Keap1/Nrf2 signal pathway. *Transl Pediatr.* 2021;10:265-75. <https://doi.org/10.21037/tp-20-200>
37. Yang M, Gao XR, Meng YN, Shen F, Chen YP. ETS1 ameliorates hyperoxia-induced alveolar epithelial cell injury by regulating the TGM2-mediated Wnt/beta-catenin pathway. *Lung.* 2021;199:681-90. <https://doi.org/10.1007/s00408-021-00489-9>
38. Tian YG, Zhang J. Protective effect of SIRT3 on acute lung injury by increasing manganese superoxide dismutase-mediated antioxidation. *Mol Med Rep.* 2018;17:5557-65. <https://doi.org/10.3892/mmr.2018.8469>
39. Reddy SP, Hassoun PM, Brower R. Redox imbalance and ventilator-induced lung injury. *Antioxid Redox Signal.* 2007;9:2003-12. <https://doi.org/10.1089/ars.2007.1770>
40. Baier RJ, Loggins J, Kruger TE. Interleukin-4 and 13 concentrations in infants at risk to develop bronchopulmonary dysplasia. *BMC Pediatr.* 2003;3:8. <https://doi.org/10.1186/1471-2431-3-8>
41. Palomer X, Roman-Azcona MS, Pizarro-Delgado J, Planavila A, Villarroja F, Valenzuela-Alcaraz B, et al. SIRT3-mediated inhibition of FOS through histone H3 deacetylation prevents cardiac fibrosis and inflammation. *Signal Transduct Target Ther.* 2020;5:14. <https://doi.org/10.1038/s41392-020-0114-1>
42. Boniakowski AM, denDekker AD, Davis FM, Joshi A, Kimball AS, Schaller M, et al. SIRT3 regulates macrophage-mediated inflammation in diabetic wound repair. *J Invest Dermatol.* 2019;139:2528-2537 e2522. <https://doi.org/10.1016/j.jid.2019.05.017>
43. Dong W, Zhu X, Liu X, Zhao X, Lei X, Kang L, et al. Role of the SENP1-SIRT1 pathway in hyperoxia-induced alveolar epithelial cell injury. *Free Radic Biol Med.* 2021;173:142-50. <https://doi.org/10.1016/j.freeradbiomed.2021.07.027>
44. Zhu X, Lei X, Wang J, Dong W. Protective effects of resveratrol on hyperoxia-induced lung injury in neonatal rats by alleviating apoptosis and ROS production. *J Matern Fetal Neonatal Med.* 2020;33:4150-58. <https://doi.org/10.1080/14767058.2019.1597846>
45. Paradies G, Paradies V, Ruggiero FM, Petrosillo G. Oxidative stress, cardiolipin and mitochondrial dysfunction in non-alcoholic fatty liver disease. *World J Gastroenterol.* 2014;20:14205-18. <https://doi.org/10.3748/wjg.v20.i39.14205>
46. Sosulski ML, Gongora R, Feghali-Bostwick C, Lasky JA, Sanchez CG. Sirtuin 3 deregulation promotes pulmonary fibrosis. *J Gerontol A Biol Sci Med Sci.* 2017;72:595-602. <https://doi.org/10.1093/gerona/glw151>
47. van de Ven RAH, Santos D, Haigis MC. Mitochondrial sirtuins and molecular mechanisms of aging. *Trends Mol Med.* 2017;23:320-31. <https://doi.org/10.1016/j.molmed.2017.02.005>
48. Xiao K, Jiang J, Wang W, Cao S, Zhu L, Zeng H, et al. Sirt3 is a tumor suppressor in lung adenocarcinoma cells. *Oncol Rep.* 2013;30:1323-8. <https://doi.org/10.3892/or.2013.2604>
49. Jin Y, Peng LQ, Zhao AL. Hyperoxia induces the apoptosis of alveolar epithelial cells and changes of pulmonary surfactant proteins. *Eur Rev Med Pharmacol Sci.* 2018;22:492-7.
50. Buccellato LJ, Tso M, Akinci OI, Chandel NS, Budinger GR. Reactive oxygen species are required for hyperoxia-induced Bax activation and cell death in alveolar epithelial cells. *J Biol Chem.* 2004;279:6753-60. <https://doi.org/10.1074/jbc.M310145200>
51. Sun W, Liu C, Chen Q, Liu N, Yan Y, Liu B. SIRT3: A new regulator of cardiovascular diseases. *Oxid Med Cell Longev.* 2018;2018:7293861. <https://doi.org/10.1155/2018/7293861>
52. Chen Y, Zhang F, Wang D, Li L, Si H, Wang C, et al. Mesenchymal stem cells attenuate diabetic lung fibrosis via adjusting Sirt3-mediated stress responses in rats. *Oxid Med Cell Longev.* 2020;2020:8076105. <https://doi.org/10.1155/2020/8076105>
53. Youle RJ, Strasser A. The BCL-2 protein family: opposing activities that mediate cell death. *Nat Rev Mol Cell Biol.* 2008;9:47-59. <https://doi.org/10.1038/nrm2308>
54. Chae YC, Kim JY, Park JW, Kim KB, Oh H, Lee KH, et al. FOXO1 degradation via G9a-mediated methylation promotes cell proliferation in colon cancer. *Nucleic Acids Res.* 2019;47:1692-705. <https://doi.org/10.1093/nar/gky1230>
55. Zhang B, Cui S, Bai X, Zhuo L, Sun X, Hong Q, et al. SIRT3 overexpression antagonizes high glucose accelerated cellular senescence in human diploid fibroblasts via the SIRT3-FOXO1 signaling pathway. *Age (Dordr).* 2013;35:2237-53. <https://doi.org/10.1007/s11357-013-9520-4>
56. Liu Y, Tong C, Xu Y, Cong P, Liu Y, Shi L, et al. CD28 deficiency ameliorates blast exposure-induced lung inflammation, oxidative stress, apoptosis, and T-cell accumulation in the lungs via the PI3K/Akt/FoxO1 signaling pathway. *Oxid Med Cell Longev.* 2019;2019:4848560. <https://doi.org/10.1155/2019/4848560>